THE JOURNAL OF PHYSICAL CHEMISTRY LETTERS
A JOURNAL OF THE AMERICAN CHEMICAL SOCIETY

pubs.acs.org/JPCL

Letter

Photodissociation of H_2S: A New Pathway for the Production of Vibrationally Excited Molecular Hydrogen in the Interstellar Medium

Yarui Zhao,[#] Junjie Chen,[#] Zijie Luo,[#] Zhenxing Li, Shuaikang Yang, Yao Chang, Feng An, Zhichao Chen, Jiayue Yang, Guorong Wu, Weiqing Zhang, Xixi Hu,* Daiqian Xie, Hongbin Ding,* Kaijun Yuan,* and Xueming Yang

Cite This: *J. Phys. Chem. Lett.* 2022, 13, 9786–9792

Read Online

ACCESS | Metrics & More | Article Recommendations | Supporting Information

ABSTRACT: Hydrogen sulfide (H_2S) is the most abundant S-bearing molecule in the solar nebula. Although its photochemistry has been studied for decades, the H_2 fragment channel is still not well-understood. Herein, we describe the photodissociation dynamics of $H_2S + h\nu \rightarrow S(^1S) + H_2(X^1\Sigma_g^+)$ with the excitation wavelength of 122 nm $\leq \lambda \leq$ 136 nm. The results reveal that the $H_2(X)$ fragments formed are significantly vibrationally excited, with the quantum yields of ~87% of $H_2(X)$ fragments populated in vibrational levels $v'' = 3$, 4, 5, and 6. Theoretical analysis suggest that these H_2 products are formed on the H_2S $4^1A'$ state surface following a nonadiabatic transition via an avoided crossing from the $3^1A'$ to $4^1A'$ state. The estimated quantum yield of the $S(^1S) + H_2$ channel is ~0.05, implying this channel should be incorporated into the appropriate interstellar chemistry models.

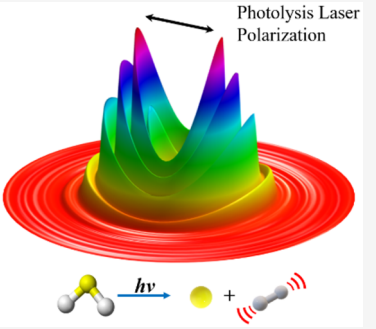

Vibrationally excited molecular hydrogen ($H_2^*(v'' > 0)$) is commonly observed in photodominated regions (PDRs) and shocked regions in the interstellar medium (ISM).[1] Since $H_2^*(v'' > 0)$ was first observed by ultraviolet spectroscopy in the atmosphere of the star ζ *Ophiuchi* in 1995,[2] an increasing number of celestial objects were reported to contain this species. This includes the HD38097 and HD199579,[3] HD147888,[4] and Herschel 36.[5] Notably, Meyer et al.[6] reported that more than 500 interstellar H_2 lines were emitted from $H_2^*(v'' = 1-14)$ from the hot star HD 37903, which is located in the NGC (New General Catalogue) 2023 reflection nebula13. The radiative lifetime of each H_2 (v'', J'') was calculated to be long (10^6–10^{12} s), which indicates the stable existence of $H_2^*(v'' > 0)$ in the ISM.[7]

In the last few decades, several studies have demonstrated that the vibrationally excited H_2 could enhance reactivity significantly, which was used to explain the long-standing problem of CH^+ formation in diffuse clouds.[8−12] The rate constant for H_2 from the $v'' = 0$ to a $v'' > 0$ state can enhance many orders of magnitude at low temperatures for the chemical reactions with an activation barrier. For instance, the rate constant enhancement for the reaction $H_2^* + C^+ \rightarrow CH^+ + H$ is as large as a factor of 10^{10} at 200 K.[13] Thus, understanding and exploring the source of interstellar $H_2^*(v'' > 0)$ is important for determining the chemical species in the ISM.

Shock waves[14−16] and far-ultraviolet (FUV) fluorescence[17] are two commonly accepted sources of interstellar H_2^*. The former means collisional excitation of H_2 molecules in shock-heated gases; while for fluorescence pumping, H_2 molecules were first excited to electronically excited states by absorption of FUV photons and then underwent radiative decay to rovibrational levels of the ground state to form $H_2^*(v'' > 0)$. Recently, an alternative source based on molecular photochemistry has been proposed. Chang et al.[18] reported that the interstellar $H_2^*(v'' > 0)$ can be directly formed from photodissociation of H_2O with the excitation wavelength in the vacuum ultraviolet (VUV) region via a competing fragmentation channel $O(^1S) + H_2(X^1\Sigma_g^+)$. The results were used to explain the green-to-red line ratio measured in comets at ~1−2 au. from the Sun.[19] In addition, France et al.[20] also proposed that water dissociation by the intense Lyman-α radiation is a possible explanation for the H_2 emission around ~1600 Å observed in the HST-COS T Tauri star. To date, however, some discrepancies between the observed H_2^* emissions and the predictions from interstellar chemistry models still exist; for example, the observed $H_2^*(v'' = 4)$ line intensities are notably stronger than the predictions.[21] Photolytic formation of H_2 is believed to be an important pathway to populate the high-energy H_2 levels in PDRs; thus, any photodissociation processes related to the H_2^* formation should be studied. In this work, we report the first observation

Received: September 7, 2022
Accepted: October 11, 2022

https://doi.org/10.1021/acs.jpclett.2c02757
J. Phys. Chem. Lett. 2022, 13, 9786−9792

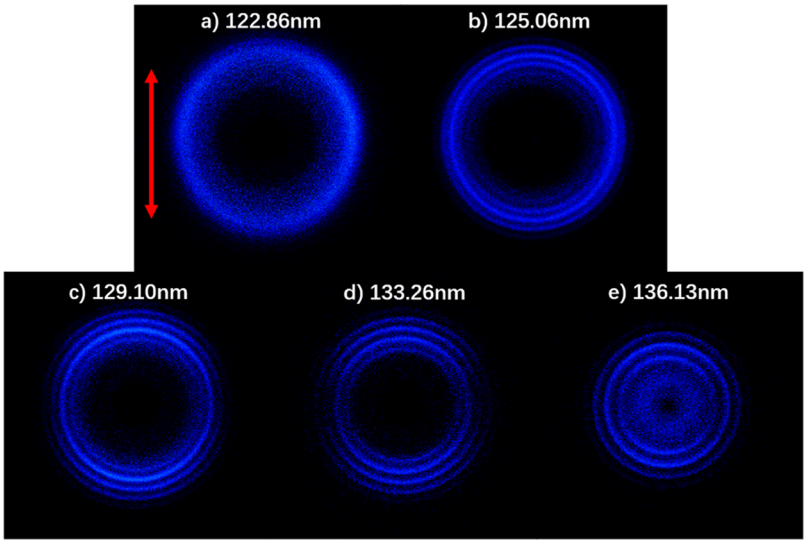

Figure 1. Time-sliced ion images of the S(^{1}S) photoproducts from photodissociation of H_2S at (a) 122.86 nm, (b) 125.06 nm, (c) 129.10 nm, (d) 133.26 nm, and (e) 136.13 nm. The red double arrow indicates the electric vector ($\boldsymbol{\varepsilon}$) of the VUV FEL. The ring features are ascribed to the vibrational states of the H_2(X, v'') coproducts.

of the fragmentation channel S(^{1}S) + H_2($X^1\Sigma_g^+$) from photodissociation of H_2S. All of the H_2 products are formed in vibrationally excited levels, which represents an alternative source of $H_2^*(v'' > 0)$ in the ISM. In addition, S(^{1}S) is also relevant to formation of carbon−sulfur species like H_2CCS and CH_3CH_2SH in carbon-rich regions.[22]

H_2S is the most abundant sulfur-bearing gas-phase species in the solar nebula, and its photodissociation has been the subject of many experimental[23−33] and theoretical[34−41] studies over the last decades. The electronic absorption spectrum of H_2S shows a weak continuous absorption band with a maximum at $\lambda \approx 195$ nm and several stronger absorption peaks with the wavelength shorter than 155 nm, which has been assigned to excitations to Rydberg states.[42−44] Excitation to the long-wavelength continuum will populate H_2S molecules into two near-degenerate states (bound $^1B_1$ and repulsive $^1A_2$ in C_{2v} symmetry, i.e., both $^1A''$ in C_s symmetry), leading to the rapid cleavage of an S−H bond and formation of the SH($X^2\Pi$) radical with minimal internal excitation.[45] At 157.6 nm photolysis, the H+SH(X) is still the dominant dissociation process.[31] In contrast, the dominant dissociation channel of H_2S at λ = 121.6 nm formed an H atom plus an electronically excited SH($A^2\Sigma$) molecule which correlates adiabatically with the $2^1A'$ surface.[32,34] Recently, systematic measurements of two main channels (H + SH and S(^{1}D) + H_2) from H_2S photolysis within the wavelength range of $122 \leq \lambda \leq 155$ nm were carried out, which provided a comprehensive picture of H_2S photofragmentation dynamics. The study revealed that the average quantum yield of SH(X) products is only about 1/4, if considering the general interstellar radiation field and the H_2S photoabsorption cross section.[46] More recently, Yuan and co-workers[47] reported quantum state-dependent dissociation dynamics of H_2S via a predissociated Rydberg state with $^1B_1$ symmetry at $\lambda \approx 139.11$ nm. This energy disposal was rationalized in terms of two competing predissociation pathways, i.e., the homogeneous (via the vibronic coupling) and heterogeneous (via the Coriolis coupling) pathways, the relative probabilities of which depend sensitively on the quantum level of parent H_2S molecules and thus on the sample temperature.

The S(^{1}S) + H_2 fragmentation channel has been demonstrated to exist in photodissociation of H_2S in earlier REMPI studies, but they provided no information about vibrational populations.[2,3,29] In this Letter, the experimental results of the S(^{1}S) + H_2 fragmentation channel from H_2S photolysis with the wavelength between 122 and 136 nm are reported. The results reveal that all of the H_2(X) fragments are significantly vibrationally excited, with the quantum yields of ∼87% of the H_2(X) fragments populated in vibrational levels $v'' = 3$, 4, 5, and 6, suggesting a new pathway for the vibrational excitation of the interstellar H_2 through molecular photochemistry.

In this study, the VUV-pump and VUV-probe method combined with the time-sliced velocity-map imaging (TS-VMI) technique was adopted. This setup has been successfully applied in photodissociation of H_2O,[48−51] CS_2,[52,53] OCS,[54,55] etc. The TS-VMI setup was equipped with two independently tunable VUV laser sources. The photolysis radiation was provided by the VUV free-electron laser (FEL) at the Dalian Coherent Light Source (DCLS),[56] which directly excited H_2S molecules to a series of predissociated Rydberg states. The subsequent S(^{1}S) products were then detected at λ = 136.13 nm (S*[$3s^23p^3(^2p^o)5s$ ($^1p^o_1$)] ← S [$3s^23p^4$ ($^1S_0$)]). This VUV radiation was generated by the difference frequency four-wave mixing ($\omega_{VUV} = 2\omega_1 - \omega_2$) method, with ω_1 = 212.556 nm and ω_2 = 486.133 nm. A pulsed supersonic molecular beam was generated by expanding a mixture of 30% H_2S in Ar through a pulsed valve. The molecular beam was perpendicular to the VUV beams. The produced S^+ ions were collected and accelerated by an ion lens and finally detected by a high-resolution VMI detector. The duration of gate voltage was set as 30 ns to acquire time-sliced ion images, and a charge-coupled device camera was used to record images on the detector.

Figure 1 displays time-sliced ion images of the S(^{1}S) fragments formed from H_2S photolysis at λ = (a) 122.86 nm, (b) 125.06 nm, (c) 129.10 nm, (d) 133.26 nm, and (e) 136.13 nm, respectively. The polarization vector of the VUV FEL, $\boldsymbol{\varepsilon}$, is indicated by a double-headed red arrow at the left top of the image. These wavelengths are located in the center of the

https://doi.org/10.1021/acs.jpclett.2c02757
J. Phys. Chem. Lett. 2022, 13, 9786−9792

strong absorption features of H_2S (Figure S1), most of which are ascribed to $nd \leftarrow 2b_1$ ($n \geq 3$) Rydberg transitions, except that the 133.26 nm is attributed to $np \leftarrow 2b_1$ ($n \geq 4$) transition. The concentric ring structures with measured relative intensities can be undoubtedly distinguished in these ion images, which is immediately assigned to the individual vibrational states of the cofragment H_2. Two other channels that could produce $S(^1S)$ photofragments are excluded, including the three-body dissociation channel (i.e., $S(^1S)$ + H + H) and the secondary dissociation of the primary SH fragment. The former is due to the photolysis photon energy being insufficient to reach its dissociation threshold ($D_{th} \geq 10.275$ eV[31]), the latter is ruled out by using an off-axis LiF lens to disperse the ω_1 and ω_2 beams from the interaction region,[47] which shows that no secondary dissociation occurs in the experiments.

The velocity distribution of the $S(^1S)$ products was determined from the radii of the resolved ring structures over all product angles in these ion images, from which the total translational energy release distributions (E_T) were derived based on conservation of momentum, as shown in Figure 2. The H_2S molecule is cooled in the supersonic

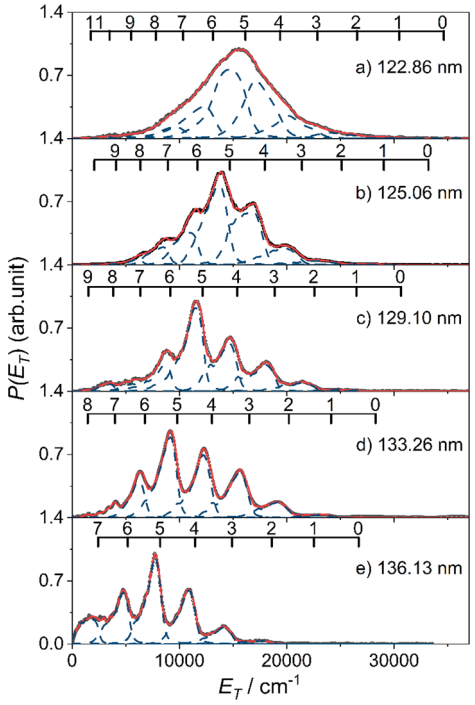

Figure 2. E_T spectra from photodissociation of H_2S at λ = (a) 122.86 nm, (b) 125.06 nm, (c) 129.10 nm, (d) 133.26 nm, and (e) 136.13 nm, along with the simulation of the spectra. The superimposed combs represent the E_T values corresponding to the formation of various $H_2(v'', J'' = 0)$.

expansion process, suggesting $E_{int}(H_2S) \approx 0$. The photon energy ($E_{h\nu}$), threshold energy (D_{th}), and internal energy of $S(^1S)$ ($E_{int}(S(^1S))$) are known constants; the internal energy of the H_2 products ($E_{int}(H_2)$) can be acquired based on energy conservation

$$E_{int}(H_2S) + E_{h\nu} - D_{th} = E_{int}(S(^1S)) + E_{int}(H_2(X)) + E_T(S(^1S) + H_2(X)) \quad (1)$$

The superposed combs in Figure 2 indicate the translational energy E_T associated with various vibrational levels of $H_2(v'', J'' = 0)$. Figure 3 displays the $H_2(X)$ vibrational state population

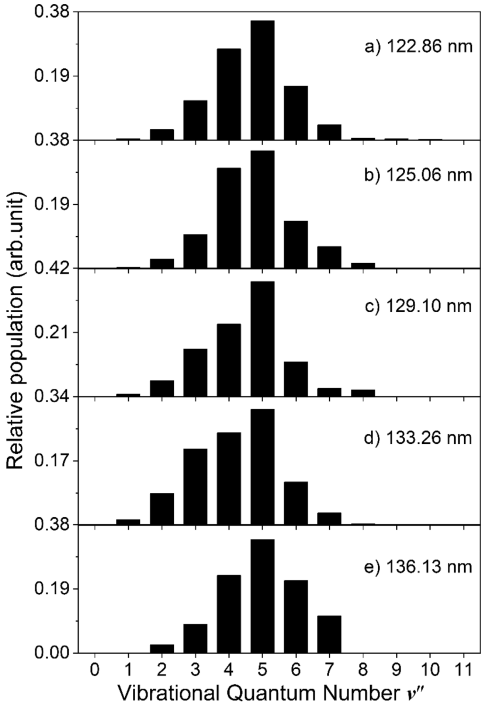

Figure 3. Vibrational state populations of $H_2(X)$ products from photodissociation of H_2S at λ = (a) 122.86 nm, (b) 125.06 nm, (c) 129.10 nm, (d) 133.26 nm, and (e) 136.13 nm.

distributions obtained by the best-fit simulation of these E_T spectra. The normalized populations are also shown in Table 1.

Table 1. Vibrational State Populations of H_2 Products from H_2S Photolysis within the Wavelength between 122 and 136 nm

$H_2(v'')$	122.86 nm	125.06 nm	129.10 nm	133.26 nm	136.13 nm
0	0	0	0	0	0
1	0.01	0	0.01	0.02	0
2	0.03	0.03	0.06	0.08	0.02
3	0.11	0.10	0.16	0.21	0.08
4	0.27	0.29	0.24	0.24	0.23
5	0.36	0.35	0.38	0.31	0.34
6	0.16	0.14	0.11	0.11	0.22
7	0.04	0.06	0.03	0.03	0.11
8	0.02	0.02	0.02		
9	0.01	0.01			
10	0.01				

The results reveal that the H_2 fragments formed from H_2S photolysis at each of the studied wavelengths show a vibrational state distribution spanning the vibrational levels of $1 \leq v'' \leq 10$, with a maximum at $v'' = 5$. In particular, about 87% of the $H_2(X)$ fragments are formed in vibrational states v'' = 3, 4, 5, and 6. The vibrational state distribution is almost independent of the photolysis wavelengths, which suggests the particular dissociation dynamics. The best fit to the vibrational profiles also reveals the rotational state population distributions of the $H_2(X, v'')$ fragments. Moderate rotational

https://doi.org/10.1021/acs.jpclett.2c02757
J. Phys. Chem. Lett. 2022, 13, 9786−9792

excitation of H_2, with the maximum population at $J'' = 5-7$, has been obtained (Figure S2).

The H_2 product spatial angular distributions can be obtained from these ion images by integrating the intensity over the corresponding radial range, which is characterized by the equation

$$I(\theta) = (1/4\pi)[1 + \beta P_2(\cos\theta)] \quad (2)$$

Here, P_2 is the second Legendre polynomial. $I(\theta)$ is the signal intensity as a function of θ, which is the angle between the recoil direction of the $S(^1S)$ products and the polarization of the VUV FEL. The angular anisotropy (β) value at the five photolysis wavelengths was determined and is shown in Table 2. It is clear that the β values change from 0.13 to 0.83 and

Table 2. Anisotropy Parameters (β Values) for H_2 Photoproducts at Five Different Photolysis Wavelengths between 122 and 136 nm

wavelength (nm)	anisotropy parameters (β)
122.86	−0.07 ± 0.03
125.06	0.06 ± 0.02
129.10	0.66 ± 0.03
133.26	0.83 ± 0.04
136.13	0.13 ± 0.06

then decrease to ∼0 when the photolysis wavelengths are varied from 136.13 to 122.86 nm, indicating that the time scale of the dissociation processes changes dramatically, which may be related to the efficiency of the nonadiabatic transition between the higher excited electronic states and the lower dissociative states. For such a central atom elimination process, the dissociation may occur via a transition state (TS) with the structure of two H atoms being on the same side of the S atom or experience two S−H bonds breaking and two H atoms recombining to form H_2, as demonstrated in CO_2[57] and H_2O[18] photodissociation. The former process is usually slow, while the latter should be relatively fast.

The energy correlation diagram of the vertical excitation of H_2S and subsequent S + H_2 fragmentation processes is shown in Figure 4. The geometric information and relative energies

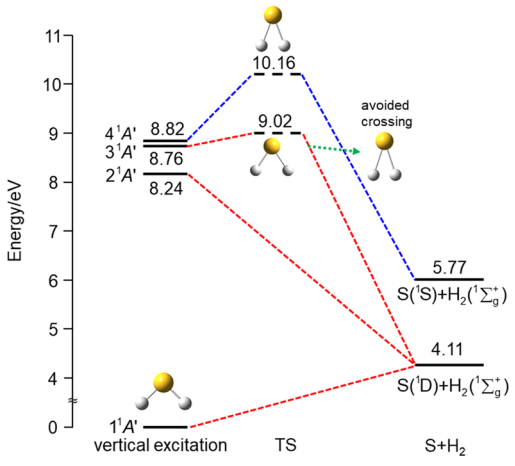

Figure 4. Correlation diagram of H_2S photodissociating to S + H_2 fragmentation for the four singlet A' electronic states. The energy of the vibrational ground state of the lowest $1^1A'$ state is taken as zero. The zero-point energy for each stationary point is considered.

including zero-point energy are obtained from the full-dimensional potential energy surfaces (PESs) for the four singlet A' electronic states of H_2S (see more detail in the Supporting Information). As shown in Figure 4, only the $4^1A'$ state adiabatically correlates with $S(^1S)$ + H_2 products, while the three lower $^1A'$ states correlate to the $S(^1D)$ + H_2 asymptote. The direct adiabatic dissociation to form $S(^1S)$ + H_2 from the $4^1A'$ state has an extremely high barrier (10.16 eV). The H_2S molecule, excited at the selected wavelengths in this study, cannot overcome this barrier. Therefore, the only way to form the $S(^1S)$ + H_2 products under the current experimental conditions must be a nonadiabatic pathway. As expected, we find an avoided crossing below 9.00 eV between the $3^1A'$ and $4^1A'$ states near the TS. The TS for the $3^1A'$ state with two S−H bonds of 1.56 Å and a quite long H−H distance of 1.72 Å shows a much lower barrier (9.02 eV) which can be overcome by the photolysis wavelength as short as 136.13 nm. The avoided crossing is located at a seam where the energies of the two states are very close and the wave functions are strongly mixed. The H−H distance for the seam is in a specified range, indicating that the product vibrational states of H_2 will span a wide distribution. As shown in Figure 5, the

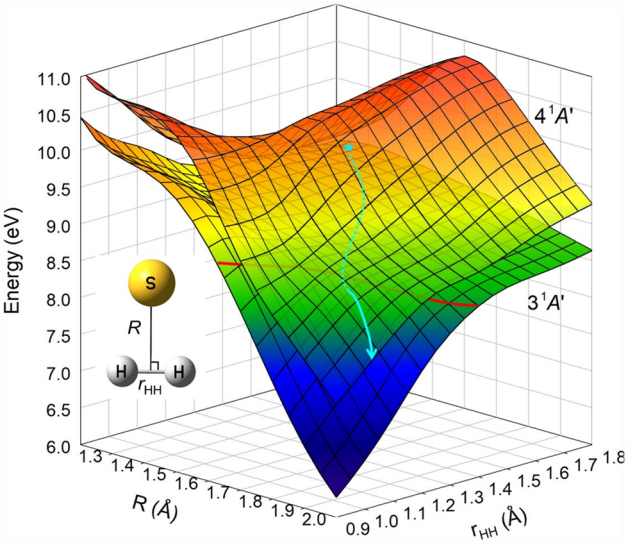

Figure 5. $3^1A'$ to $4^1A'$ adiabatic PESs as functions of the R and r_{HH} in S + H_2 Jacobi coordinates with the angle fixed at 90°. The aqua star on the $3^1A'$ PES is the transition state. The red line displays the crossing seam between the two states. The cyan pathway illustrates the nonadiabatic dissociation process forming the $S(^1S)$ + H_2 products.

smallest energy difference, which means the strongest state-mixing, appears when both S−H bonds increase to ∼1.80 Å and the H−H separation decreases to ∼1.1 Å. As shown in our previous work,[18] the average bond length of H_2 ($v'' = 5$) is 1.1 Å. This might be the reason why $H_2(v'' = 5)$ is most abundant at all of the photolysis wavelengths in these experiments. In addition, for shorter wavelengths, the higher available energy facilitates the nonadiabatic transition through larger H−H bond lengths, leading to H_2 formation in higher vibrational levels, which is also consistent with the experimental results. Thus, for H_2S photolysis at λ = 122.86−136.13 nm, the molecule undergoes a fast internal conversion from the initial excited Rydberg state to the $3^1A'$ state, and then the $S(^1S)$ atoms in conjunction with H_2^* ($v''>0$) cofragments are formed

https://doi.org/10.1021/acs.jpclett.2c02757
J. Phys. Chem. Lett. 2022, 13, 9786−9792

on the $4^1A'$ state surface following a nonadiabatic transition though the avoided crossing from the $3^1A'$ to the $4^1A'$ state, wherein the two H atoms get close and the S−H bond elongates.

As mentioned above, vibrationally excited H_2 is a crucial species in the ISM due to its high reactivity. Recent observations showed that the $H_2^*(v'' > 0)$ have notable populations in highly excited vibrational levels, which cannot be fully understood by collisional excitation or the FUV fluorescence mechanisms.[20] The $H_2^*(v'' > 0)$ formation from molecular photochemistry or chemical reactions must be responsible for an apparent excess of H_2 in the high vibrational levels. Our previous study revealed the vibrationally excited H_2 was formed from H_2O photodissociation, which suggested an additional budget of $H_2^*(v'' > 0)$ in the ISM.[18] This work presents evidence for the vibrational excitation of H_2 in the $S(^1S) + H_2$ channel from H_2S photodissociation, which implies another source of the interstellar $H_2^*(v'' > 0)$.

The quantitative assessment of the importance of VUV photodissociation of H_2S and its role in the $H_2^*(v''>0)$ formation in the ISM requires determination of the quantum yield of the $S(^1S) + H_2$ channel. Such measurements are beyond the scope of this study. In our previous studies, we have both measured the translational energy spectra of the H and $S(^1D)$ atoms from H_2S photolysis with the wavelength between 122 and 155 nm and provided an estimated quantum yield ($\leq$0.12) of the $S(^1D) + H_2$ products at λ = 139.11 nm.[46] At shorter wavelengths, the quantum yield of the $S(^1D) + H_2$ channel should be not far from 0.12, since the $S(^1D)$ + 2H channel becomes important as the photolysis wavelength decreases. In this work, we have measured the $S(^1S)$ and $S(^1D)$ fragments under the same experimental conditions at these VUV photolysis wavelengths. The calibration of the $S(^1S)$ and $S(^1D)$ detection efficiencies shows that the quantum yield of the $S(^1S) + H_2$ channel is $\leq$0.05 at these wavelengths, with ±50% uncertainty due to the complicated calibration process (see Figure S3 and more detail in the Supporting Information). Given the high abundance of H_2S molecules in the ISM, the photodissociation of H_2S induced by the interstellar radiation field are expected to form considerable $H_2^*(v'' > 0)$ and thus should be incorporated in the interstellar chemistry model, in addition to H_2O photodissociation.[18]

In summary, we have studied the fragmentation dynamics of $H_2S + h\nu \rightarrow S(^1S) + H_2(X^1\Sigma_g^+)$ at the state-to-state level. The formed H_2 fragments show a wide distribution of vibrational states with a peak at $v'' = 5$. Though this dissociation process is minor, the prominent production of $H_2^*(v'' > 0)$ from H_2S photolysis is likely to have a role in the PDRs. Given the similar behavior of H_2O and H_2S, we propose that this vibrationally excited H_2 channel should be general in the photodissociation of hydrogen-containing interstellar molecules, which should inspire scientists to search for more unexpected photochemical processes.

■ ASSOCIATED CONTENT

Supporting Information

The Supporting Information is available free of charge at https://pubs.acs.org/doi/10.1021/acs.jpclett.2c02757.

Detailed description of the experimental methods and theoretical methods; Figures S1−S4; Tables S1 and S2 (PDF)

■ AUTHOR INFORMATION

Corresponding Authors

Xixi Hu − *Kuang Yaming Honors School, Institute for Brain Sciences, Jiangsu Key Laboratory of Vehicle Emissions Control, Center of Modern Analysis, Nanjing University, Nanjing 210023, China;* orcid.org/0000-0003-1530-3015; Email: xxhu@nju.edu.cn

Hongbin Ding − *School of Physics, Key Laboratory of Materials Modification by Laser, Ion and Electron Beams, Chinese Ministry of Education, Dalian University of Technology, Dalian 116024, China*; Email: hding@dlut.edu.cn

Kaijun Yuan − *State Key Laboratory of Molecular Reaction Dynamics and Dalian Coherent Light Source, Dalian Institute of Chemical Physics, Chinese Academy of Sciences, Dalian 116023, China; Hefei National Laboratory, Hefei 230088, China;* orcid.org/0000-0002-5108-8984; Email: kjyuan@dicp.ac.cn

Authors

Yarui Zhao − *School of Physics, Key Laboratory of Materials Modification by Laser, Ion and Electron Beams, Chinese Ministry of Education, Dalian University of Technology, Dalian 116024, China; State Key Laboratory of Molecular Reaction Dynamics and Dalian Coherent Light Source, Dalian Institute of Chemical Physics, Chinese Academy of Sciences, Dalian 116023, China*

Junjie Chen − *Institute of Theoretical and Computational Chemistry, Key Laboratory of Mesoscopic Chemistry, School of Chemistry and Chemical Engineering Nanjing University, Nanjing 210093, China*

Zijie Luo − *State Key Laboratory of Molecular Reaction Dynamics and Dalian Coherent Light Source, Dalian Institute of Chemical Physics, Chinese Academy of Sciences, Dalian 116023, China*

Zhenxing Li − *State Key Laboratory of Molecular Reaction Dynamics and Dalian Coherent Light Source, Dalian Institute of Chemical Physics, Chinese Academy of Sciences, Dalian 116023, China*

Shuaikang Yang − *State Key Laboratory of Molecular Reaction Dynamics and Dalian Coherent Light Source, Dalian Institute of Chemical Physics, Chinese Academy of Sciences, Dalian 116023, China*

Yao Chang − *State Key Laboratory of Molecular Reaction Dynamics and Dalian Coherent Light Source, Dalian Institute of Chemical Physics, Chinese Academy of Sciences, Dalian 116023, China*

Feng An − *Institute of Theoretical and Computational Chemistry, Key Laboratory of Mesoscopic Chemistry, School of Chemistry and Chemical Engineering Nanjing University, Nanjing 210093, China*

Zhichao Chen − *State Key Laboratory of Molecular Reaction Dynamics and Dalian Coherent Light Source, Dalian Institute of Chemical Physics, Chinese Academy of Sciences, Dalian 116023, China*

Jiayue Yang − *State Key Laboratory of Molecular Reaction Dynamics and Dalian Coherent Light Source, Dalian Institute of Chemical Physics, Chinese Academy of Sciences, Dalian 116023, China*

Guorong Wu − *State Key Laboratory of Molecular Reaction Dynamics and Dalian Coherent Light Source, Dalian Institute of Chemical Physics, Chinese Academy of Sciences,*

https://doi.org/10.1021/acs.jpclett.2c02757
J. Phys. Chem. Lett. 2022, 13, 9786−9792

Dalian 116023, China; orcid.org/0000-0002-0212-183X

Weiqing Zhang − *State Key Laboratory of Molecular Reaction Dynamics and Dalian Coherent Light Source, Dalian Institute of Chemical Physics, Chinese Academy of Sciences, Dalian 116023, China*

Daiqian Xie − *Institute of Theoretical and Computational Chemistry, Key Laboratory of Mesoscopic Chemistry, School of Chemistry and Chemical Engineering Nanjing University, Nanjing 210093, China;* orcid.org/0000-0001-7185-7085

Xueming Yang − *State Key Laboratory of Molecular Reaction Dynamics and Dalian Coherent Light Source, Dalian Institute of Chemical Physics, Chinese Academy of Sciences, Dalian 116023, China; Hefei National Laboratory, Hefei 230088, China; Department of Chemistry, College of Science, Southern University of Science and Technology, Shenzhen 518005, China;* orcid.org/0000-0001-6684-9187

Complete contact information is available at: https://pubs.acs.org/10.1021/acs.jpclett.2c02757

Author Contributions

#Y. Zhao, J. Chen, and Z. Luo contributed equally to this work.

Notes

The authors declare no competing financial interest.

■ ACKNOWLEDGMENTS

We thank the National Natural Science Foundation of China (Grant Nos. 21922306, 22225303, 22122302, 12047532, and 51837008, and the NSFC Center for Chemical Dynamics (Grant No. 22288201)), the Key Technology Team of the Chinese Academy of Sciences (Grant No. GJJSTD20220001), the Innovation Program for Quantum Science and Technology (2021ZD0303304), and the Liaoning Revitalization Talents Program (Grant No. XLYC1907154). Y. Chang is supported by the Special Research Assistant Funding Project of Chinese Academy of Sciences and the China Postdoctoral Science Foundation (Grant No. 2021M693118). X. Yang thanks the Guangdong Science and Technology Program (Grant Nos. 2019ZT08L455 and 2019JC01X091) and the Shenzhen Science and Technology Program (Grant No. ZDSYS20200421111001787). We thank Prof. M. N. R. Ashfold for helpful discussions and the staff team of the Dalian Coherent Light Source (DCLS) for technical support.

■ REFERENCES

(1) Wakelam, V.; Bron, E.; Cazaux, S.; Dulieu, F.; Gry, C.; Guillard, P.; Habart, E.; Hornekaer, L.; Morisset, S.; Nyman, G.; Pirronello, V.; Price, S. D.; Valdivia, V.; Vidali, G.; Watanabe, N. H_2 formation on interstellar dust grains: the viewpoints of theory, experiments, models and observations. *Mol. Astrophys.* **2017**, *9*, 1−36.

(2) Federman, S. R.; Cardell, J. A.; Vandishoeck, E. F.; Lambert, D. L.; Black, J. H. Vibrationally excited H_2, HCl, and NO^+ in the diffuse clouds toward zeta-ophiuchi. *Astrophys. J.* **1995**, *445*, 325−329.

(3) Jensen, A. G.; Snow, T. P.; Sonneborn, G.; Rachford, B. L. Observational properties of rotationally excited molecular hydrogen in translucent lines of sight. *Astrophys. J.* **2010**, *711*, 1236−1256.

(4) Gnacinski, P. Interstellar H_2 toward HD 147888. *Astron. Astrophys.* **2013**, *549*, A37.

(5) Rachford, B. L.; Snow, T. P.; Ross, T. L. Vibrationally excited molecular hydrogen near herschel 36. *Astrophys. J.* **2014**, *786*, 159.

(6) Meyer, D. M.; Lauroesch, J. T.; Sofia, U. J.; Draine, B. T.; Bertoldi, F. The rich ultraviolet spectrum of vibrationally excited interstellar H_2 toward HD 37903. *Astrophys. J.* **2001**, *553*, L59−L62.

(7) Roueff, E.; Abgrall, H.; Czachorowski, P.; Pachucki, K.; Puchalski, M.; Komasa, J. The full infrared spectrum of molecular hydrogen. *Astron. Astrophys.* **2019**, *630*, A58.

(8) Stecher, T. P.; Williams, D. A. CH and CH^+ formation in ion−molecule reactions. *Astrophys. J.* **1972**, *177*, L141−L148.

(9) Freeman, A.; Williams, D. A. Vibrationally excited molecular hydrogen in circumstellar clouds and the interstellar CH^+ abundance. *Astrophys. Space Sci.* **1982**, *83*, 417−422.

(10) Douglas, A. E.; Herzberg, G. CH^+ in interstellar space and in the laboratory. *Astrophys. J.* **1941**, *94*, 381−381.

(11) Hierl, P. M.; Morris, R. A.; Viggiano, A. A. Rate coefficients for the endothermic reactions $C^+(^2P)+H_2(D_2)\rightarrow CH^+(CD^+)+H(D)$ as functions of temperature from 400−1300 K. *J. Chem. Phys.* **1997**, *106*, 10145−10152.

(12) Jones, M. E.; Barlow, S. E.; Ellison, G. B.; Ferguson, E. E. Reactions of C^+, He^+, and Ne^+ with vibrationally excited H_2 and D_2. *Chem. Phys. Lett.* **1986**, *130*, 218−223.

(13) Agundez, M.; Goicoechea, J. R.; Cernicharo, J.; Faure, A.; Roueff, E. The chemistry of vibrationally excited H_2 in the interstellar medium. *Astrophys. J.* **2010**, *713*, 662−670.

(14) Gautier, T. N.; Fink, U.; Treffers, R. R.; Larson, H. P. Detection of molecular hydrogen quadrupole emission in Orion nebula. *Astrophys. J.* **1976**, *207*, L129−L133.

(15) Kwan, J.; Scoville, N. Nature of broad molecular line emission at kleinmann-low nebula. *Astrophys. J.* **1976**, *210*, L39−L43.

(16) Beckwith, S.; Persson, S. E.; Neugebauer, G.; Becklin, E. E. Observations of molecular hydrogen emission from Orion nebula. *Astrophys. J.* **1978**, *223*, 464−470.

(17) Gatley, I.; Hasegawa, T.; Suzuki, H.; Garden, R.; Brand, P.; Lightfoot, J.; Glencross, W.; Okuda, H.; Nagata, T. Fluorescent molecular hydrogen emission from the reflection nebula NGC 2023. *Astrophys. J., Lett. Ed. (USA)* **1987**, *318*, 73−76.

(18) Chang, Y.; An, F.; Chen, Z. C.; Luo, Z. J.; Zhao, Y. R.; Hu, X. X.; Yang, J. Y.; Zhang, W. Q.; Wu, G. R.; Xie, D. Q.; Yuan, K. J.; Yang, X. M. Vibrationally excited molecular hydrogen production from the water photochemistry. *Nat. Commun.* **2021**, *12*, 6303.

(19) Kawakita, H. Photodissociation rate, excess energy, and kinetic total energy release for the photolysis of H_2O producing $O(^1S)$ by solar UV radiation field. *Astrophys. J.* **2022**, *931*, 24.

(20) France, K.; Roueff, E.; Abgrall, H. The 1600 angstrom emission bump in protoplanetary disks: A spectral signature of H_2O dissociation. *Astrophys. J.* **2017**, *844*, 169.

(21) Burton, M. G.; Bulmer, M.; Moorhouse, A.; Geballe, T. R.; Brand, P. W. J. L. Fluorescent molecular hydrogen line emission in the far-red. *Mon. Not. R. Astron. Soc.* **1992**, *257*, 1P.

(22) Shingledecker, C. N.; Banu, T.; Kang, Y.; Wei, H. J.; Wandishin, J.; Nobis, G.; Jarvis, V.; Quinn, F.; Quinn, G.; Molpeceres, G.; Mccarthy, M. C.; Mcguire, B. A.; Kaestner, J. Grain surface hydrogen addition reactions as a chemical link between cold cores and hot corinos: The case of H_2CCS and CH_3CH_2SH. *J. Phys. Chem. A* **2022**, *126*, 5343−5353.

(23) Hawkins, W. G.; Houston, P. L. 193 nm photodissociation of H_2S: the SH internal energy distribution. *J. Chem. Phys.* **1980**, *73*, 297−302.

(24) Hawkins, W. G.; Houston, P. L. Rotational distributions in the photodissociation of bent triatomics: H_2S. *J. Chem. Phys.* **1982**, *76*, 729−731.

(25) Vanveen, G. N. A.; Mohamed, K. A.; Baller, T.; Devries, A. E. Photofragmentation of H_2S in the first continuum. *Chem. Phys.* **1983**, *74*, 261−271.

(26) Xu, Z.; Koplitz, B.; Wittig, C. Kinetic and internal energy distributions via velocity aligned doppler spectroscopy: The 193 nm photodissociation of H_2S and HBr. *J. Chem. Phys.* **1987**, *87*, 1062−1069.

(27) Kleinermanns, K.; Linnebach, E.; Suntz, R. Emission spectrum of dissociating H_2S. *J. Phys. Chem.* **1987**, *91*, 5543−5545.

(28) Weiner, B. R.; Levene, H. B.; Valentini, J. J.; Baronavski, A. P. Ultraviolet photodissociation dynamics of H_2S and D_2S. *J. Chem. Phys.* **1989**, *90*, 1403−1414.

(29) Steadman, J.; Baer, T. The production and spectroscopy of excited sulfur atoms from the two-photon dissociation of H_2S. *J. Chem. Phys.* **1988**, *89*, 5507−5513.
(30) Morley, G. P.; Lambert, I. R.; Mordaunt, D. H.; Wilson, S. H. S.; Ashfold, M. N. R.; Dixon, R. N.; Western, C. M. Translational spectroscopy of H(D) atom fragments arising from the photodissociation of $H_2S(D_2S)$: A redetermination of D_0(S-H). *J. Chem. Soc. Faraday Trans.* **1993**, *89*, 3865−3875.
(31) Liu, X.; Hwang, D. W.; Yang, X. F.; Harich, S.; Lin, J. J.; Yang, X. Photodissociation of hydrogen sulfide at 157.6 nm: Observation of SH bimodal rotational distribution. *J. Chem. Phys.* **1999**, *111*, 3940−3945.
(32) Schnieder, L.; Meier, W.; Welge, K. H.; Ashfold, M. N. R.; Western, C. M. Photodissociation dynamics of H_2S at 121.6 nm and a determination of the potential energy function of $SH(A\ ^2\Sigma^+)$. *J. Chem. Phys.* **1990**, *92*, 7027−7037.
(33) Lai, K. F.; Beyer, M.; Salumbides, E. J.; Ubachs, W. Photolysis production and spectroscopic investigation of the highest vibrational states in H_2 ($X^1\Sigma_g^+$, v = 13, 14). *J. Phys. Chem. A* **2021**, *125*, 1221−1228.
(34) Cook, P. A.; Langford, S. R.; Dixon, R. N.; Ashfold, M. N. R. An experimental and ab initio reinvestigation of the Lyman-alpha photodissociation of H_2S and D_2S. *J. Chem. Phys.* **2001**, *114*, 1672−1684.
(35) Kulander, K. C. The photodissociation of H_2S: A study of indirect photodissociation. *Chem. Phys. Lett.* **1984**, *103*, 373−377.
(36) Theodorakopoulos, G.; Petsalakis, I. D. Asymmetric dissociation and bending potentials of H_2S in the ground and excited electronic states. *Chem. Phys. Lett.* **1991**, *178*, 475−482.
(37) Theodorakopoulos, G.; Petsalakis, I. D.; Nicolaides, C. A. Diabatic potentials for the 1 ^{1}A" and 2 ^{1}A" states of H_2S. *Chem. Phys. Lett.* **1993**, *207*, 321−324.
(38) Heumann, B.; Weide, K.; Duren, R.; Schinke, R. Nonadiabatic effects in the photodissociation of H_2S in the first absorption band: An ab initio study. *J. Chem. Phys.* **1993**, *98*, 5508−5525.
(39) Heumann, B.; Schinke, R. Emission spectroscopy of dissociating H_2S: Influence of nonadiabatic coupling. *J. Chem. Phys.* **1994**, *101*, 7488−7499.
(40) Simah, D.; Hartke, B.; Werner, H. J. Photodissociation dynamics of H_2S on new coupled ab initio potential energy surfaces. *J. Chem. Phys.* **1999**, *111*, 4523−4534.
(41) Palenikova, J.; Kraus, M.; Neogrady, P.; Kello, V.; Urban, M. Theoretical study of molecular properties of low-lying electronic excited states of H_2O and H_2S. *Mol. Phys.* **2008**, *106*, 2333−2344.
(42) Masuko, H.; Morioka, Y.; Nakamura, M.; Ishiguro, E.; Sasanuma, M. Absorption spectrum of the H_2S molecule in the vacuum ultraviolet region. *Can. J. Phys.* **1979**, *57*, 745−759.
(43) Lee, L. C.; Wang, X. Y.; Suto, M. Quantitative photoabsorption and fluorescence spectroscopy of H_2S and D_2S at 49−240 nm. *J. Chem. Phys.* **1987**, *86*, 4353−4361.
(44) Mayhew, C. A.; Connerade, J. P.; Baig, M. A.; Ashfold, M. N. R.; Bayley, J. M.; Dixon, R. N.; Prince, J. D. High resolution studies of the electronic spectra of H_2S and D_2S. *J. Chem. Soc. Faraday Trans.* **1987**, *83*, 417−434.
(45) Wilson, S. H. S.; Howe, J. D.; Ashfold, M. N. R. On the near ultraviolet photodissociation of hydrogen sulphide. *Mol. Phys.* **1996**, *88*, 841−858.
(46) Zhou, J. M.; Zhao, Y. R.; Hansen, C. S.; Yang, J. Y.; Chang, Y.; Yu, Y.; Cheng, G. K.; Chen, Z. C.; He, Z. G.; Yu, S. R.; Ding, H. B.; Zhang, W. Q.; Wu, G. R.; Dai, D. X.; Western, C. M.; Ashfold, M. N. R.; Yuan, K. J.; Yang, X. M. Ultraviolet photolysis of H_2S and its implications for SH radical production in the interstellar medium. *Nat. Commun.* **2020**, *11*, 1547.
(47) Zhao, Y. R.; Luo, Z. J.; Chang, Y.; Wu, Y. C.; Zhang, S. E.; Li, Z. X.; Ding, H. B.; Wu, G. R.; Campbell, J. S.; Hansen, C. S.; Crane, S. W.; Western, C. M.; Ashfold, M. N. R.; Yuan, K. J.; Yang, X. M. Rotational and nuclear-spin level dependent photodissociation dynamics of H_2S. *Nat. Commun.* **2021**, *12*, 4459.
(48) Chang, Y.; Li, Q.; An, F.; Luo, Z.; Zhao, Y.; Yu, Y.; He, Z.; Chen, Z.; Che, L.; Ding, H.; Zhang, W.; Wu, G.; Hu, X.; Xie, D.; Plane, J. M. C.; Feng, W.; Western, C. M.; Ashfold, M. N. R.; Yuan, K.; Yang, X. Water photolysis and its contributions to the hydroxyl dayglow emissions in the atmospheres of Earth and Mars. *J. Phys. Chem. Lett.* **2020**, *11*, 9086−9092.
(49) Chang, Y.; He, Z. G.; Luo, Z. J.; Zhou, J. M.; Zhang, Z. G.; Chen, Z. C.; Yang, J. Y.; Yu, Y.; Li, Q. M.; Che, L.; Wu, G. R.; Wang, X. A.; Yang, X. M.; Yuan, K. J. Application of laser dispersion method in apparatus combining H atom Rydberg tagging time-of-flight technique with vacuum ultraviolet free electron laser. *Chin. J. Chem. Phys.* **2020**, *33*, 139−144.
(50) Chang, Y.; Yu, Y.; Wang, H. L.; Hu, X. X.; Li, Q. M.; Yang, J. Y.; Su, S.; He, Z. G.; Chen, Z. C.; Che, L.; Wang, X. N.; Zhang, W. Q.; Wu, G. R.; Xie, D. Q.; Ashfold, M. N. R.; Yuan, K. J.; Yang, X. M. Hydroxyl super rotors from vacuum ultraviolet photodissociation of water. *Nat. Commun.* **2019**, *10*, 1250.
(51) Chang, Y.; Yu, Y.; An, F.; Luo, Z.; Quan, D.; Zhang, X.; Hu, X.; Li, Q.; Yang, J.; Chen, Z.; Che, L.; Zhang, W.; Wu, G.; Xie, D.; Ashfold, M. N. R.; Yuan, K.; Yang, X. Three body photodissociation of the water molecule and its implications for prebiotic oxygen production. *Nat. Commun.* **2021**, *12*, 2476.
(52) Li, Z.; Zhao, M.; Xie, T.; Luo, Z.; Chang, Y.; Cheng, G.; Yang, J.; Chen, Z.; Zhang, W.; Wu, G.; Wang, X.; Yuan, K.; Yang, X. Direct observation of the C + S_2 channel in CS_2 photodissociation. *J. Phys. Chem. Lett.* **2021**, *12*, 844−849.
(53) Zhao, M.; Li, Z.; Xie, T.; Chang, Y.; Wu, F.; Wang, Q.; Chen, W.; Wang, T.; Wang, X.; Yuan, K.; Yang, X. Photodissociation dynamics of CS_2 near 204 nm: The $S(^3P)$+$CS(X^1\sum^+)$ channels. *Chin. J. Chem. Phys.* **2021**, *34*, 95−101.
(54) Chen, W.; Zhang, L.; Yuan, D.; Chang, Y.; Yu, S.; Wang, S.; Wang, T.; Jiang, B.; Yuan, K.; Yang, X.; Wang, X. Observation of the carbon elimination channel in vacuum ultraviolet photodissociation of OCS. *J. Phys. Chem. Lett.* **2019**, *10*, 4783−4787.
(55) Xie, T.; Chen, W.; Yuan, D.; Yu, S.; Fu, B.; Yuan, K.; Yang, X.; Wang, X. Photodissociation dynamics of OCS near 150 nm: The $S(^1S_{J=0})$ and $S(^3P_{J=2,1,0})$ product channels. *J. Phys. Chem. A* **2020**, *124*, 6420−6426.
(56) Chang, Y.; Yu, S.; Li, Q.; Yu, Y.; Wang, H.; Su, S.; Chen, Z.; Che, L.; Wang, X.; Zhang, W.; Dai, D.; Wu, G.; Yuan, K.; Yang, X. Tunable VUV photochemistry using vacuum ultraviolet free electron laser combined with H-atom Rydberg tagging time-of-flight spectroscopy. *Rev. Sci. Instrum.* **2018**, *89*, No. 063113.
(57) Wang, X. D.; Gao, X. F.; Xuan, C. J.; Tian, S. X. Dissociative electron attachment to CO_2 produces molecular oxygen. *Nat. Chem.* **2016**, *8*, 258−263.

https://doi.org/10.1021/acs.jpclett.2c02757
J. Phys. Chem. Lett. 2022, 13, 9786−9792